MSCA Doctorate Network

CONTRABASS

zero-CO_2 cemeNt ThRough cArBonation of cAlcium Silicates and aluminateS

Deliverable D2.1

SiO_2–CaO–Al_2O_3–CO_2–H_2O system speciation

Funded by the European Union

Funded by the European Union. Views and opinions expressed are however those of the author(s) only and do not necessarily reflect those of the European Union or the European Research Executive Agency (REA). Neither the European Union nor the granting authority can be held responsible for them.

Grant Agreement N°	101119715
Project name	Zero-CO2 cemeNt THrough cArBonation of cAlcium Silicates and aluminates
Project acronym	CONTRABASS
Topic	HORIZON-MSCA-2022-DN-01-01
Call (part) identifier	HORIZON-MSCA-2022-DN-01
Starting date	01/01/2024
Type of action	HORIZON TMA MSCA Doctoral Networks
Granting authority	European Research Executive Agency
Start date of the project	01 January 2024
Project duration	48 months
Project coordinator	Hegoi Manzano (UPV/EHU)

Deliverable N°	D2.1
Deliverable name	SiO_2–CaO–Al_2O_3–CO_2–H_2O system speciation
WP N°	WP2
WP Leader	Christophe Labbez
Author	Jeswin Jiji
Contributors	Jeswin Jiji, Christophe Labbez
Due date	Month 21 (September 2025)
Actual submission date	Month 24 (December 2025)
Dissemination level	PU

This project has received funding from the European Union's Horizon Europe research and innovation programme under Grant Agreement No 101119715.

Funded by the European Union

Funded by the European Union. Views and opinions expressed are however those of the author(s) only and do not necessarily reflect those of the European Union or the European Research Executive Agency (REA). Neither the European Union nor the granting authority can be held responsible for them.

Document history		
Revision	**Date**	**Description**
1	24/11/2025	First draft
2	28/11/2025	Second draft
3	3/12/2025	Final revision

Report contributors		
Name	**Beneficiary short name**	**Details of contribution**
Jeswin Jiji	UBE	Preparation of first draft and revisions
Christophe Labbez	CNRS	Preparation of second draft and revisions

Disclaimer

The information in this document is provided "as is", and no guarantee or warranty is given that the information is fit for any particular purpose. The content of this document reflects only the author's view. The European Research Executive Agency (REA) is not responsible for any use that may be made of the information it contains. The users use the information at their sole risk and liability. The content of this report does not reflect the official opinion of the European Research Executive Agency (REA). Responsibility for the information and views expressed in this report lies entirely with the author(s).

Funded by the European Union

Funded by the European Union. Views and opinions expressed are however those of the author(s) only and do not necessarily reflect those of the European Union or the European Research Executive Agency (REA). Neither the European Union nor the granting authority can be held responsible for them.

Contents

1 Executive Summary **5**

2 Abbreviations and acronyms **6**

3 Background **7**

4 Objective **8**

5 Literature review and choice of experimental dataset **10**

6 Methodology **14**

6.1 Thermodynamic Definitions 14

6.2 Microscopic model and simulations of silicates 16

6.3 Model Parameters Optimization 18

6.3.1 NaCl aqueous solution 18

6.3.2 H^+ and OH^- 18

6.3.3 Orthosilicic acid 19

6.3.4 Intrinsic pK 20

6.3.5 Bond length 22

6.4 Oligomerization constant 23

7 Results **25**

8 Thermodynamic database **26**

9 Conclusions **29**

A Appendix **32**

A.1 Comparison of PHREEQC Speciation with Potentiometric and ^{29}Si NMR Data . . 32

A.2 Standard errors and fit quality 33

Funded by the European Union

Funded by the European Union. Views and opinions expressed are however those of the author(s) only and do not necessarily reflect those of the European Union or the European Research Executive Agency (REA). Neither the European Union nor the granting authority can be held responsible for them.

1 Executive Summary

The present deliverable focuses on the thermodynamic modelling of silicate speciation in solution, which remains one of the main gaps in the thermodynamic modelling of the SiO_2–Al_2O_3–CO_2–H_2O system and, more broadly, in the solution chemistry of one of the most important element in the Earth's crust. The main reason for this gap is that current speciation models, also known as geochemical models, which are all based on the mean–field theory of electrolytic solutions (Debye–Hückel theory, etc.), ignore intramolecular interactions, which for charged polysilicates can be significant and vary significantly with the ionic strength of the medium. In other words, these classical approaches do not allow intrinsic acid dissociation constants K_a^{int} for polysilicates to be obtained, but rather effective constants K_a^{eff} that can be highly dependent on ionic strength I. Unfortunately, due to the complexity of silicate speciation, $K_a^{\text{eff}} = f(I)$ values for all deprotonation reactions of all polysilicates cannot be obtained from experimental measurements alone.

In this work, the problem is solved by developing a microscopic model of polysilicates within the framework of the primitive model. The model explicitly accounts for intra- and extra-molecular interactions as well as microscopic protonation and deprotonation reactions of silicates. The model is solved by Monte Carlo simulations in the grand canonical ensemble and the titration scheme introduced by Labbez *et al.* [1]. The model parameters were set against independent experimental data and use the assumption that the intrinsic microscopic acid dissociation constant of the silanol function is constant regardless of the degree of oligomerization of the polysilicates. The simulation results are then averaged out into macroscopic $K_a^{\text{eff}}(I)$ for silicate oligomers to be used in classical geochemical models. Using this original methodology, a thermodynamic database for classical geochemical models is provided for polysilicates up to tetramers, valid in a relatively large pH and ionic strength range, i.e. $0 < \text{pH} < 12$,and $0 < I < 2\,\text{M}$ (DOI: 10.5281/zenodo.17791184).

The current database does not yet include the second ionization of the silicate monomers of the polysilicates and complexation with calcium. This, together with polysilicates with a higher degree of polymerization, will be included in future database versions. It should be noted that despite its current limitations, the existing database has been validated against experimental data and should be sufficient to provide an accurate description of silicate speciation under carbonation conditions. More generally, the original methodology introduced could easily be transferred to other chemistries, whether aluminates or the large family of organic polymers.

Funded by the European Union

Funded by the European Union. Views and opinions expressed are however those of the author(s) only and do not necessarily reflect those of the European Union or the European Research Executive Agency (REA). Neither the European Union nor the granting authority can be held responsible for them.

2 Abbreviations and acronyms

Abbreviation	Description
K_a^{int}	Intrinsic acid dissociation constant.
K_a^{app}	Apparent acid dissociation constant.
K_a^{eff}	Effective acid dissociation constant.
I	Ionic strength.
IAP	Ion activity product.
β_{pq}	Apparent polysilicate formation constant.
MC	Monte Carlo simulation.
PHREEQC	Geochemical speciation code.
CEMDATA18	Cement thermodynamic database.
Q^n	^{29}Si NMR connectivity notation.
C–S–H	Calcium silicate hydrate.
C–(A)–S–H	Calcium alumino-silicate hydrate.

Funded by the European Union

Funded by the European Union. Views and opinions expressed are however those of the author(s) only and do not necessarily reflect those of the European Union or the European Research Executive Agency (REA). Neither the European Union nor the granting authority can be held responsible for them.

3 Background

The present document constitutes the Deliverable D2.1 "SiO_2–CaO–Al_2O_3–CO_2–H_2O System Speciation" in the framework of the Marie Skłodowska–Curie Actions Doctoral Network Project 101119715 – CONTRABASS as described in the HORIZON-MSCA-2022-DN-01.

Funded by the European Union

Funded by the European Union. Views and opinions expressed are however those of the author(s) only and do not necessarily reflect those of the European Union or the European Research Executive Agency (REA). Neither the European Union nor the granting authority can be held responsible for them.

4 Objective

Carbon mineralization is a practical route for permanent CO_2 sequestration. In this process CO_2 reacts with calcium or magnesium containing phases to form solid carbonate minerals that remain stable over geological timescales. In the cement industry, carbon mineralization can be obtained by carbon curing of cement clinker or accelerated carbonation of hydrated cement fines coming from recycling concrete-made infrastructure and housing. During the carbonation of hydrated cement, the cement hydrates dissolves and re-precipitate as $CaCO_3$ together with an alumino–silica gel. By capturing and converting CO_2 during these processs, the CO_2 emissions associated with cement production is reduced, lowering the overall carbon footprint of the material.

A rate controlling factor in the carbonation process is the dissolution of the main cement hydrate, that is calcium silicate hydrate (C–(A)–S–H). The latter is driven by the degree of undersaturation in the pore solution. Undersaturation is quantified by the ratio of the ion activity product (IAP) of dissolved species to the solubility product (K_s) of the solid phase. When IAP $<$ K_s, the solution is undersaturated and C–(A)–S–H dissolves. Evaluation of the IAP depends on an accurate description of aqueous species constituting C–(A)–S–H. However, the silicate speciation [2, 3] is so far not accurately described by classical thermodynamic modelling. The main objective of this deliverable is to provide an accurate thermodynamic database for silicate speciation under the conditions relevant to cement carbonation.

In aqueous alkaline media orthosilicic acid $Si(OH)_4$ undergoes pH-dependent deprotonation and oligomerization reactions, forming dimers, trimers, and larger polymeric silicates which in turn deprotonate. Equilibria which define deprotonation states are strongly modulated by ionic strength and solution composition.

Despite extensive research, the thermodynamic modelling of silicate speciation remains limited, with large spreads in reported equilibrium constants. Geochemical models (e.g., PHREEQC or GEMS with CEMDATA databases) rely on mean-field theories of electrolyte solutions (Debye–Hückel, Davies, Pitzer) which are not well suited for the description of charged oligomers and polymers as they do not account for the intramolecular electrostatic repulsion arising from the charged monomers.

To overcome this limitation, we employ a microscopic model solved with Monte-Carlo simulations that explicitly incorporates intramolecular electrostatic interactions. The model is able to describe accurately the silicate speciation at T = 298 K and P = 1 atm and for a large range of

Funded by the European Union

Funded by the European Union. Views and opinions expressed are however those of the author(s) only and do not necessarily reflect those of the European Union or the European Research Executive Agency (REA). Neither the European Union nor the granting authority can be held responsible for them.

pH and ionic strength conditions, i.e. $0 \leq \text{pH} \leq 12$ and $0 \leq \text{I} \leq 2\text{M}$.

The results from the microscopic model are finally average out to produce *effective* equilibrium constants to be used in classical thermodynamic modelling that effectively account for the intramolecular electrostatic interaction, to reproduce the silicate speciation. The later are tabulated into a thermodynamic database that can be directly imported into standard geochemical modelling tools such as PHREEQC or GEMS.

Funded by the European Union

Funded by the European Union. Views and opinions expressed are however those of the author(s) only and do not necessarily reflect those of the European Union or the European Research Executive Agency (REA). Neither the European Union nor the granting authority can be held responsible for them.

5 Literature review and choice of experimental dataset

Silicate chemistry/speciation, in aqueous solution is governed by four processes: (i) pH-dependent deprotonation of silicic acid, $Si(OH)_4$ (ii) condensation reactions that generate oligomeric silicate species (iii) titration of oligomeric silicate species and eventually (iv) complexation of the silicate species with simple ions.

Deprotonation of silanols occurs through stepwise acid–base equilibria of the general form

$$Si_qO_xH_y^p \rightleftharpoons H^+ + Si_qO_xH_{y-1}^{p-1},$$

where q is the number of silicon atoms, x is the number of oxygen atoms, y is the number of silanol groups, and p is the total charge of the species. These reactions govern the charge state of silicate species under alkaline conditions.

Oligomerization (condensation) proceeds through the general reaction.

$$q\,Si(OH)_4 \rightleftharpoons Si_qO_{4q-m}H_{4q-2m} + m\,H_2O,$$

Where q denotes the number of $Si(OH)_4$ monomers involved in the condensation, and m is the number of Si–O–Si linkages formed (equivalently, the number of H_2O molecules released). And these reactions generates dimers, trimers, and larger polysilicate species depending on the extent of condensation.

To provide a unified thermodynamic description of both deprotonation and oligomerization, Sjöberg and co-workers adopted the general silicate formation equilibrium

$$p\,H^+ + q\,Si(OH)_4 \rightleftharpoons (H^+)_p[Si(OH)_4]_q,$$

with formation constant β_{pq}. Here q denotes the number of silicon atoms in the oligomer and p is the charge of the species. This notation allows all condensed and deprotonated oligomers to be represented consistently within a single equilibrium reaction.

Table 1 summarizes the values of $\log \beta_{pq}$ reported in the literature. The wide spread of reported values illustrates the difficulty of establishing a thermodynamic model. This spread, as we will see later, can be explained mainly by the high variability of the measured equilibrium constants with the ionic strength and modelling used as reported in in Table 2 . In fact, experimentally only *apparent* constants can be obtained, defined by the product of concentrations (for a definition see

Funded by the European Union

Funded by the European Union. Views and opinions expressed are however those of the author(s) only and do not necessarily reflect those of the European Union or the European Research Executive Agency (REA). Neither the European Union nor the granting authority can be held responsible for them.

the methodology section), as there is no simple way to measure the chemical activities of each silicate species.

On the other hand, the thermodynamic modelling relies on mean field theory where the point like description of all species, including the silicate oligomers, ignore the internal electrostatic repulsions within oligo-silicates carrying multiple charges, i.e., the intramolecular electrostatic interaction. And, these repulsions vary with the ionic strength of the medium. As we will see, this problem can be solved by introducing an *effective* equilibrium constant that varies with ionic strength.

In this study we use the dataset of apparent equilibrium constants of Sjöberg *et al.* [2], wherein silicate oligomers and ionization state were quantified through a careful combination of ^{29}Si NMR and potentiometric titrations. These measurements align closely with the concentration and chemical conditions relevant to the present work, making the dataset a basis for benchmarking and model parametrization.

Funded by the European Union

Funded by the European Union. Views and opinions expressed are however those of the author(s) only and do not necessarily reflect those of the European Union or the European Research Executive Agency (REA). Neither the European Union nor the granting authority can be held responsible for them.

Table 1: Reported *apparent* and *effective* $\log \beta_{pq}$ for silica oligomers relative to $Si(OH)_4(aq)$ from experimental and modeling studies, respectively.

p, q	[4]	[5]	[6]	[7]	[2]	[8]	[9]	[3]	[10]	[11]	[12]
0,2					1.3	2.52				2.7	1.2
1,2	-6.46				-7.75		-8.1	-5.0 / -0.10	-8.50, -8.14, -7.86, -7.65	-7.1	-8.50
2,2	-16.26	-18.12			-18.00		-19.0	-18.0 / -0.06		-19.8	-19.4
3,2	-29.06										
4,2								-42.1 / -0.58			
3,3					-26.43 / -25.40		-28.6 / -27.5	-25.2 / -0.33	-29.40, -28.75, -28.34, -28.11	-28.6	-29.3 / -29.4
6,3								-63.0 / -0.90			
0,3										5.4	6.21
1,3										-4.4	
2,3										-15.3	
0,4										8.1	
1,4										-1.7	
2,4		-12.57	-12.37	-13.44				-8.9 / -0.17		-11.5	-15.6
4,4		-32.48		-35.80	-32.81		-34.9	-32.5 / -0.51		-37.7	-39.2 / -39.1
8,4								-84.1 / -1.17			
0,6										13.5	
1,6										3.7	
2,6										-6.1	
3,6										-15.9	
4,6								-25.0 / -0.53		-30.3	
5,6										-44.3	
6,6								47.6 / -0.94			-61.8
0,8										18.9	
1,8										9.1	
2,8										-0.7	
3,8										-10.5	
4,8										-20.3	
5,8										-35.7	
6,8								-38.0 / -1.00			
8,8								-64.0 / -1.17			
16,32								-65.4 / -2.55			

Funded by the European Union

Funded by the European Union. Views and opinions expressed are however those of the author(s) only and do not necessarily reflect those of the European Union or the European Research Executive Agency (REA). Neither the European Union nor the granting authority can be held responsible for them.

Table 2: Summary of ionic strength and methodology for the references in Table 1.

Reference	Ionic strength / medium	Experimental or modelling approach
Roller (1940) [4]	Alkaline NaOH solutions, moderate to high ionic strength	Solubility and emf measurements for silica in base
Lagerström (1959) [5]	0.5–3 M $NaClO_4$	Potentiometric titration of silicic acid and dimers at fixed I
Ingri (1959) [6]	NaCl and $NaClO_4$ media, $I < 1$ M	Acid–base titrations, evaluation of monomer deprotonation and small oligomers
Baes and Mesmer (1976) [7]	Mixed electrolyte datasets, extrapolated to $I \to 0$	Davies equation for activity coefficients
Sjöberg et al. (1985) [2]	NaCl, $I \approx 0.6$ M, 25 °C	Potentiometry plus ^{29}Si NMR. monomer, dimer, cyclic trimer, cyclic tetramer identified and fitted
Applin (1987) [8]	Alkaline NaOH–silica systems	Solubility and transport measurements.
NEA (1989) [9]	Reference state $I = 0$	Critical review. recommended intrinsic constants
Svensson et al. (1986) [3]	Concentrated Na silicate	Glass electrode potentiometry and quantitative ^{29}Si NMR
Xiong (2013) [10]	High ionic strength brines	Pitzer modelling of solubility, emf, and speciation data
Gaboriaud et al. (1999) [11]	Na silicate, high I	Pitzer reinterpretation of ^{29}Si NMR distributions
Felmy et al. (1999) [12]	Brines up to several molal	Pitzer parametrization implemented in geochemical models

Funded by the European Union

Funded by the European Union. Views and opinions expressed are however those of the author(s) only and do not necessarily reflect those of the European Union or the European Research Executive Agency (REA). Neither the European Union nor the granting authority can be held responsible for them.

6 Methodology

A microscopic model was constructed to describe silicate speciation in electrolyte solutions. The model was developed in the framework of the primitive model where all ions are considered explicitly while water is treated as a dielectric continuum, characterized by its dielectric permittivity, $\epsilon_r = 78.5$ (at room temperature). Besides the charges, the primitive model contains yet another parameter and that is the hard core radius of the ions. The silicate oligomers are modelled by n beads connected by jointed rigid bonds. The ions were modelled as charged hard spheres and the beads by titratable hard spheres. The model uses the ionic diameters, σ of H^+, Na^+ and Cl^- parametrized by Abbas et al [13]. Which allows to accurately describe the mean ion activity of NaCl and HCl aqueous solutions up to respectively 1M and 2 M. σ_{OH} was parametrized to reproduce the variation of the apparent autoprotolysis equilibrium constant with the ionic strength. The bead size and the bond length of the silicate oligomers were parametrized to reproduce the apparent equilibrium constant of Sjoberg for silicic acid at various ionic strength and silicate dimers in 0.6 M NaCl solution. The model further assumes that the microscopic *intrinsic* acid dissociation constant of the silanol function, $pK^{\text{int}}_{a,SiOH}$ is constant whatever the size of silicate oligomers. The oligomerization constants of silicates are then obtained to reproduce the experimental $\log \beta_{p,q}$ of Sjoberg et al.

The microscopic model is solved with Monte Carlo simulations in the grand canonical ensemble at constant pH using the titration move developed by Labbez et al.[1]. The simulations were use to generate ionization curves and species distributions for mono and polysilicic acids over a large range of ionic strengths and pH. Finally, the simulation results were average out into macroscopic[1] *effective* acid dissociation constants for silicate oligomers that can be directly used in classical thermodynamic calculations such as with PHREEQC or GEMS software.

6.1 Thermodynamic Definitions

For the sake of clarity we start to provide the definition of intrinsic, apparent and effective equilibrium acid dissociation constants before to jump to the description of the model and simulations. We use as an example the first ionization constant of silicic acid and the second ionization constant of a silicate dimer.

[1] we mean here by macroscopic the pK^{eff}_a to be defined at the level of the molecule to distinguish it from the microscopic pK_a of the silanol function

Funded by the European Union

Funded by the European Union. Views and opinions expressed are however those of the author(s) only and do not necessarily reflect those of the European Union or the European Research Executive Agency (REA). Neither the European Union nor the granting authority can be held responsible for them.

Given the first acid dissociation reaction of silicic acid,

$$\mathrm{Si(OH)_4} \rightleftharpoons \mathrm{Si(OH)_3O^-} + \mathrm{H^+},$$

the intrinsic acid dissociation constant of the reaction is defined as

$$K_a^{\mathrm{int}} = \frac{a(\mathrm{Si(OH)_3O^-})\, a(\mathrm{H^+})}{a(\mathrm{Si(OH)_4})}.$$

the chemical activity product of the products over that of the reactants to the power of their stoichiometric coefficient. Activities of species i are related to their concentrations through

$$a_i = \gamma_i\, c_i,$$

where $\gamma_i = \exp(\beta \mu_i^{ex})$ denotes the activity coefficient and μ_i^{ex} the excess chemical potential.

Apparent constants $\mathrm{K_a^{app}}(I)$ are obtained from the measurement of the equilibrium concentrations of products and reactant and are related to $\mathrm{K_a^{int}}$ by,

$$\mathrm{K_a^{int}} = \mathrm{K_a^{app}}(I)\, \frac{\gamma_{\mathrm{Si(OH)_3O^-}}\, \gamma_{\mathrm{H^+}}}{\gamma_{\mathrm{Si(OH)_4}}}.$$

It is good to mention here that $\log(\gamma_{\mathrm{H^+}})$ is nothing but the difference between the thermodynamic pH $(-\log(a_{\mathrm{H^+}}))$ and the measured apparent pH $(-\log(c_{\mathrm{H^+}}))$. One can also note that $\mathrm{p}K_{\mathrm{a}}^{\mathrm{app}}$ is ionic strength and temperature dependent.

Let us now introduce the effective constant concept taking as an example the second ionization reaction of a silicate dimer,

$$(\mathrm{Si(OH)_3})\mathrm{O}(\mathrm{Si(OH)_2^-}) \rightleftharpoons (\mathrm{Si(OH)_2^-})\mathrm{O}(\mathrm{Si(OH)_2^-}) + \mathrm{H^+},$$

In this case the effective Gibbs free energy difference can be written as

$$\Delta G^{\mathrm{eff}} = \Delta G^{\mathrm{int}} + \Delta G^{\mathrm{el}},$$

where $\Delta G^{\mathrm{int}} = -RT \ln K_a^{\mathrm{int}}$, $\Delta G^{\mathrm{eff}} = -RT \ln K_a^{\mathrm{eff}}$ and ΔG^{el} is the electrostatic free energy cost to

Funded by the European Union

Funded by the European Union. Views and opinions expressed are however those of the author(s) only and do not necessarily reflect those of the European Union or the European Research Executive Agency (REA). Neither the European Union nor the granting authority can be held responsible for them.

ionize the second monomer. This defines the macroscopic *effective* equilibium constant that can be used in classical thermodynamic modelling (i.e. PHREEQC or GEMS) to *effectively* account for the intramolecular interactions. Note that we mean by macroscopic pK, the pK at the level of the silicate oligomer to distinguish it from the microscopic pK at the level of the sites or monomers.

The macroscopic pK^{eff} are obtained from solutions of the microscopic model. As an example, for a dimer where we only consider the first ionization of the two silicate monomers, the microscopic free energy of microstate $\mathrm{n} = (n_1, n_2)$ where

$$n_i = \begin{cases} 0, & \text{if monomer } i \text{ is protonated (Si–(OH)}_3\text{)}, \\ 1, & \text{if monomer } i \text{ is deprotonated (Si–(OH)}_2\text{O}^-\text{)}. \end{cases}$$

gives,

$$G(\mathbf{n};\mathrm{pH}) = \ln(10)\, RT \sum_{i=1}^{2} \Big(\mathrm{p}K_a^{\text{int}} - \mathrm{pH}\Big)\, n_i \;+\; \frac{1}{2}\sum_{i\neq j} J_{ij}\, n_i n_j.$$

where J_{ij} is the electrostatic interaction free energy between monomers i and j.

6.2 Microscopic model and simulations of silicates

Orthosilicic acid is represented by a single titratable hard spheres, with charge 0, -1 or -2 depending on its deprotonation state. Silicate oligomers are built by linking titratable beads together with rigid bonds, forming either linear chains or closed cyclic structures depending on their topology Fig. 1.

The bond length and angles between beads are kept fixed throughout the simulation.

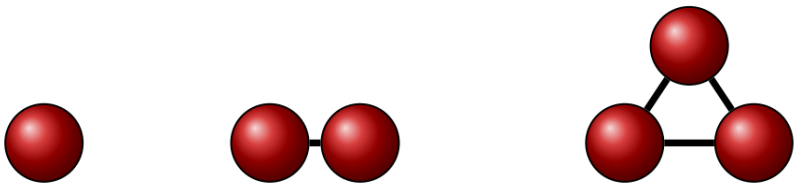

Figure 1: Coarse grained monomer, dimer, and cyclic trimer.

The species interact through two pairwise interaction potentials, that is a hard core potential

Funded by the European Union

Funded by the European Union. Views and opinions expressed are however those of the author(s) only and do not necessarily reflect those of the European Union or the European Research Executive Agency (REA). Neither the European Union nor the granting authority can be held responsible for them.

and a Coulomb potential. Hard sphere exclusion prevents overlap and fixes the minimum approach distance between the species and is defined as,

$$U_{\mathrm{HS}}(r) = \begin{cases} \infty, & r < \sigma_{ij}, \\ 0, & r \geq \sigma_{ij}. \end{cases}$$

where σ_{ij} denotes the hard-sphere contact distance between coarse grained spheres i and j.

Electrostatic interactions between species i and j of charge q separated a distance r are described by a pair-wise Coulomb potential screened by the dielectric constant of water, ε_r.

$$U_{\mathrm{C}}(r) = \frac{q_i q_j}{4\pi\varepsilon_0\varepsilon_r r}.$$

The simulation box length, with periodic boundary condition, was chosen so that the equilibrated system contained a few hundred Na^+ and Cl^- ions, ensuring bulk-like salt behaviour (Fig. 2). The minimum image convention was used.

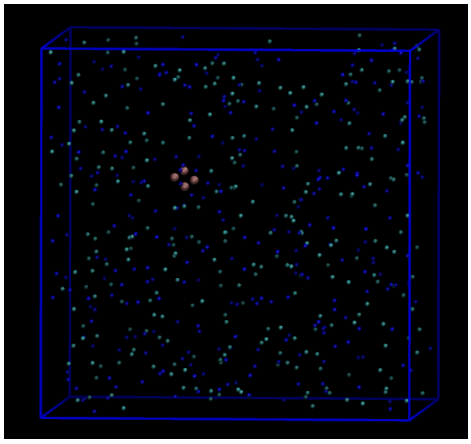

Figure 2: Simulation box of a silicate tetramer constructed from monomer units (shown in pink), surrounded by sodium (blue) and chloride (green) ions. The tetramer is placed in a cubic simulation cell under periodic boundary conditions.

The model was solved with Monte Carlo (MC) simulations, using the Faunus open source code [14, 15], in the grand canonical ensemble using the titration scheme introduced by Labbez and Jönsson [1]. Deprotonation and protonation events are proposed at random sites and accepted with a Metropolis criterion depending on the intrinsic pK_{a}, the imposed pH, and the electrostatic

Funded by the European Union

Funded by the European Union. Views and opinions expressed are however those of the author(s) only and do not necessarily reflect those of the European Union or the European Research Executive Agency (REA). Neither the European Union nor the granting authority can be held responsible for them.

energy change upon adding or removing a proton. This algorithm allows direct sampling of pH-dependent equilibria while maintaining charge neutrality through counter ion compensation.

Simulations are run at set temperature and chemical potential of the salt for the desired ionic strength with one single silicate species centred in the simulation box. By scanning pH, species distributions as a function of their charge state for each ionic strength are obtained. From the α(pH) curves, where α is defined as the fraction of ionized silicate species relative to the total amount of silicate, the apparent pK_{a} values (pH at half-neutralization) for each deprotonation reaction of silicate species are calculated.

For each pH value, the system was equilibrated with 5×10^3 MC cycles followed by production runs of 5×10^4 MC cycles. In a MC cycle, a translation move for each species, 100 titration moves, and 100 grand canonical moves were attempted.

6.3 Model Parameters Optimization

6.3.1 NaCl aqueous solution

A well validated primitive model for NaCl aqueous solution from Abbas et al. [13] was used in this work, where $r_{\mathrm{Na}} = 1.58$ Å and $r_{\mathrm{Cl}} = 1.91$ Å. These ion radii were treated as fixed input parameters throughout the study. The model reproduces with high accuracy the mean ion activity of the NaCl solution for $0 \leq I \leq 1$M.

6.3.2 H^+ and OH^-

To obtain a reliable description of proton activity and pH in Monte Carlo simulations, the radii of H^+ and OH^- were optimized using the ionic-strength dependence of the apparent autoprotolysis constant of water, p$K_w^{\mathrm{app}}(I)$ together with the parametrized size of H^+ obtained by Abbas et al to reproduce the mean ion activity of HCl aqueous solutions. The optimal radii, $r_{\mathrm{H}} = 2.10$ Å and $r_{\mathrm{OH}} = 1.63$ Å, were obtained as those fitting the experimental p$K_w^{\mathrm{app}}(I)$ data reported in studies [6, 16–19], as shown in Fig. 3.

Funded by the European Union

Funded by the European Union. Views and opinions expressed are however those of the author(s) only and do not necessarily reflect those of the European Union or the European Research Executive Agency (REA). Neither the European Union nor the granting authority can be held responsible for them.

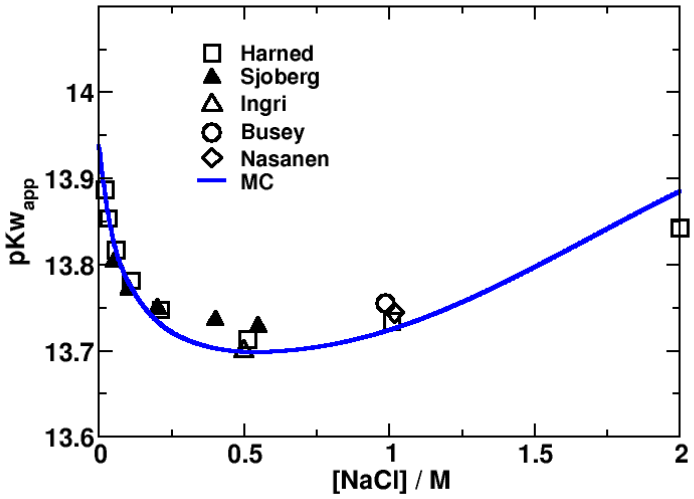

Figure 3: $\mathrm{p}K_w^{\mathrm{app}}$ as a function of NaCl concentration. Symbols represent experimental literature values from refs [6, 16–19]. The blue curve corresponds to the values obtained from Monte Carlo simulations using the optimized H^+ and OH^- radii.

6.3.3 Orthosilicic acid

The $\mathrm{p}K_{\mathrm{a}}^{\mathrm{app}}(I)$ for the first deprotonation of H_4SiO_4,

$$H_4SiO_4 \rightleftharpoons H_3SiO_4^- + H^+,$$

was used to determine the optimal size of the H_4SiO_4 particle in the model. The radius $r_{H_4SiO_4}$ was adjusted so that the simulated $\mathrm{p}K_{\mathrm{a}}^{\mathrm{app}}(I)$ for the first deprotonation of orthosilicic acid matched the ionic-strength dependence measured experimentally by Sjöberg [18]. The best agreement was obtained with $r_{H_4SiO_4} = 1.53$ Å as shown in (Fig. 4).

Funded by the European Union

Funded by the European Union. Views and opinions expressed are however those of the author(s) only and do not necessarily reflect those of the European Union or the European Research Executive Agency (REA). Neither the European Union nor the granting authority can be held responsible for them.

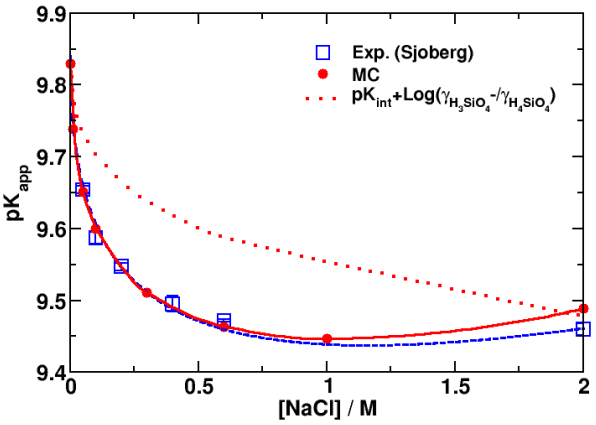

Figure 4: $\mathrm{p}K_{\mathrm{a}}^{\mathrm{app}}(I)$ of first ionisation of orthosilicic acid as a function of NaCl concentration. Blue symbols: experimental data from Sjöberg. Red points: Monte Carlo results using the optimized H_4SiO_4 radius.

6.3.4 Intrinsic pK

The $\mathrm{p}K_{\mathrm{a}}^{\mathrm{int}}$ for the monomers to be used in the simulations were obtained by assuming that the microscopic intrinsic constant for the first ionisation of the silanol function, $\mathrm{p}K_{\mathrm{a}}^{\mathrm{int}}(=\mathrm{Si–OH})$ is constant whatever the size of the oligomer,

$$= \mathrm{Si}-\mathrm{OH} \rightleftharpoons = \mathrm{Si}-\mathrm{O}^- + \mathrm{H}^+,$$

The average charge of a silicic acid molecule is defined by the probability to find each of the four silanol groups in a deprotonated microstate at a given pH, $\langle Q \rangle = 4p(\mathrm{pH})$ which by definition is

$$\langle Q \rangle = -4 \left[\frac{1}{1 + 10^{\mathrm{p}K_a^{\mathrm{int}}(=\mathrm{Si–OH})-\mathrm{pH}}} \right],$$

Similarly it can be easily shown that from the macroscopic reaction of silicic acid,

$$\mathrm{Si(OH)_4} \rightleftharpoons \mathrm{Si(OH)_3O^-} + \mathrm{H^+},$$

Funded by the European Union

Funded by the European Union. Views and opinions expressed are however those of the author(s) only and do not necessarily reflect those of the European Union or the European Research Executive Agency (REA). Neither the European Union nor the granting authority can be held responsible for them.

the macroscopic intrinsic ionisation constant reads,

$$K_a^{\text{int}}(\text{H}_4\text{SiO}_4) = \frac{a_{\text{Si(OH)}_3\text{O}^-} a_{\text{H}^+}}{a_{\text{Si(OH)}_4}} = 4(\,10^{\,\text{pH}-\text{p}K_a^{\text{int}}(=\text{Si–OH})}) \cdot a_{\text{H}^+}$$

due to the four charge microstates of the four silanol functions of the silicic molecules. It then comes that,

$$\text{p}K_a^{\text{int}}(=\text{Si}-\text{OH}) = \text{p}K_a^{\text{int}}(\text{H}_4\text{SiO}_4) + \log_{10} 4$$

providing $\text{p}K_a^{\text{int}}(=\text{Si}-\text{OH}) = 10.43$ given $\text{p}K_a^{\text{int}}(\text{H}_4\text{SiO}_4) = 9.83$.

For any species whose first deprotonation can occur through n charge microstates, the corresponding intrinsic molecular acidity is therefore

$$\text{p}K_{\text{a}}^{\text{int}}(\text{silicate oligomer}) = \text{p}K_{\text{a}}^{\text{int}}(=\text{Si}-\text{OH}) - \log_{10}(n).$$

from which pK_a^{int}(silicate monomer) needed for the simulations can be calculated. The latter is provided in Fig. 5 as a function of the oligomerization degree and geometry. Observable differences in $\text{p}K_{\text{a}}^{\text{int}}$ between monomers and oligomers therefore arise from the increasing number of accessible charge microstates at larger degrees of oligomerization.

Funded by the European Union

Funded by the European Union. Views and opinions expressed are however those of the author(s) only and do not necessarily reflect those of the European Union or the European Research Executive Agency (REA). Neither the European Union nor the granting authority can be held responsible for them.

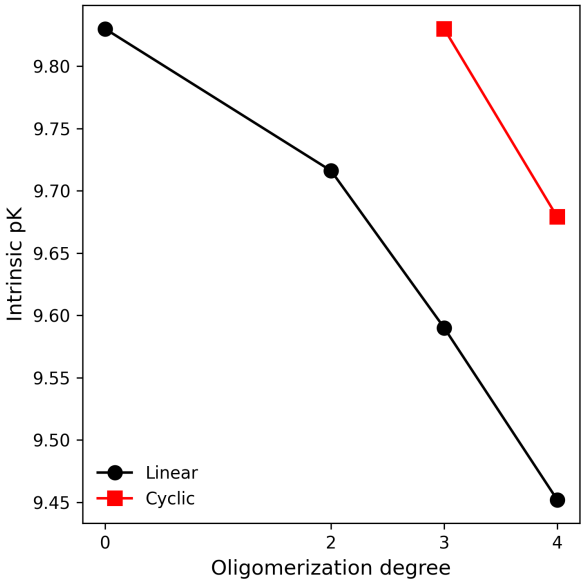

Figure 5: Intrinsic acid dissociation constant, $\mathrm{p}K_{\mathrm{a}}^{\mathrm{int}}$ per Si monomers as a function of oligomerization degree for linear and cyclic poly-silicates.

6.3.5 Bond length

The bond length of the microscopic model for oligomers was determined from the silicate dimer. The microscopic model for the dimer contains a single Si–Si bond, and from Sjöberg we have the corresponding equilibrium constants measured experimentally at 0.6 M.

$$2\,\mathrm{H_4SiO_4} \rightleftharpoons \mathrm{H_6Si_2O_8} + \mathrm{H_2O}, \qquad \log\beta_{0,2} = 1.30,$$

$$2\,\mathrm{H_4SiO_4} \rightleftharpoons \mathrm{H_4Si_2O_7^{2-}} + 2\,\mathrm{H^+} + H_2O, \qquad \log\beta_{-2,2} = -18.0$$

Simulations with the silicate dimer were performed at 0.6 M NaCl at various bond length using the previously determined ion radii and the intrinsic acid dissociation constant determined in the previous section. For each imposed distance, the corresponding $\log\beta_{-2,2}$ was computed and compared with the experimental one.

The Si–Si separation that reproduced the experimental value best is $L_{\mathrm{Si\text{–}Si}} = 3.0$ Å(Fig. 6) with $\mathrm{p}K_{a1}^{\mathrm{app}}(\mathrm{H_6Si_2O_7})_{0.6M} = 9.05$ and $\mathrm{p}K_{a2}^{\mathrm{app}}(\mathrm{H_5Si_2O_7^-})_{0.6M} = 9.25$ in very good agreement with Sjöberg experimental values.

Funded by the European Union

Funded by the European Union. Views and opinions expressed are however those of the author(s) only and do not necessarily reflect those of the European Union or the European Research Executive Agency (REA). Neither the European Union nor the granting authority can be held responsible for them.

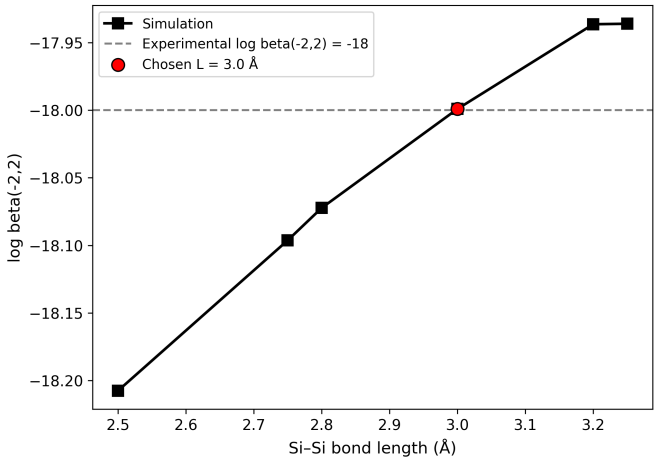

Figure 6: Variation of $\log \beta_{-2,2}$ with Si–Si bond length.

6.4 Oligomerization constant

The required oligomerization constant for the various oligomers was calculated from the simulated $\mathrm{p}K_a^{\mathrm{app}}(\mathrm{oligomers})_{0.6M}$ and Sjöberg's experimentally determined $\log_{10} \beta_{p,q}$ at the same ionic strength. We recall here that $\log_{10} \beta_{p,q}$ is the sum of the oligomerization constant and the apparent ionization constant, see the definition provided in the literature review section. The obtained oligomerization constant are provided in Fig. 7.

Funded by the European Union

Funded by the European Union. Views and opinions expressed are however those of the author(s) only and do not necessarily reflect those of the European Union or the European Research Executive Agency (REA). Neither the European Union nor the granting authority can be held responsible for them.

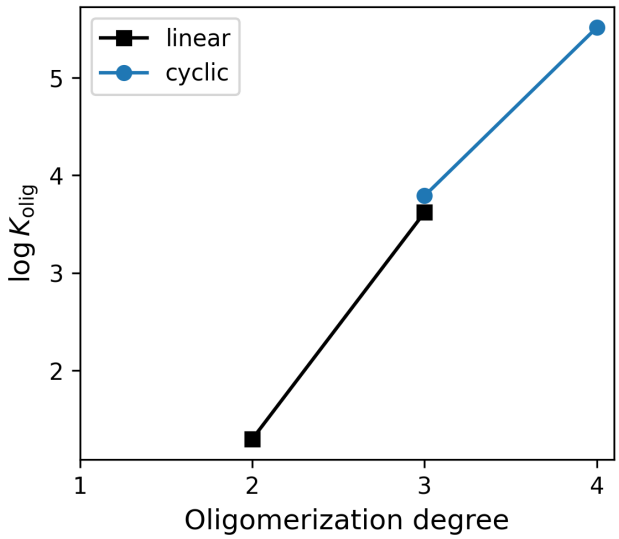

Figure 7: Oligomerization equilibrium constants $\log K$ as a function of oligomerization degree. Obtained from the Monte Carlo derived $\mathrm{p}K_{\mathrm{a}}^{\mathrm{app}}(I)$ values (Fig. 8).

Funded by the European Union

Funded by the European Union. Views and opinions expressed are however those of the author(s) only and do not necessarily reflect those of the European Union or the European Research Executive Agency (REA). Neither the European Union nor the granting authority can be held responsible for them.

7 Results

Monte Carlo simulations were used to extract the macroscopic $pK_a^{app}(I)$for the oligomers from the simulated titration curves. Across monomeric and oligomeric silicates, $pK_a^{app}(I)$ decreases monotonically with increasing ionic strength. This behaviour reflects the reduction of electrostatic repulsion caused by increased screening and the corresponding decrease of the Debye–Hückel length.

Conversely, for higher deprotonation steps (e.g. transitions from -1 to -2, -2 to -3, etc.), $pK_a^{app}(I)$ increases due to additional negative charges within the same oligomer enhancing intramolecular electrostatic repulsion. These two behaviours are illustrated in Fig. 8 for a silicate tetramer and are consistently observed for all oligomer sizes studied.

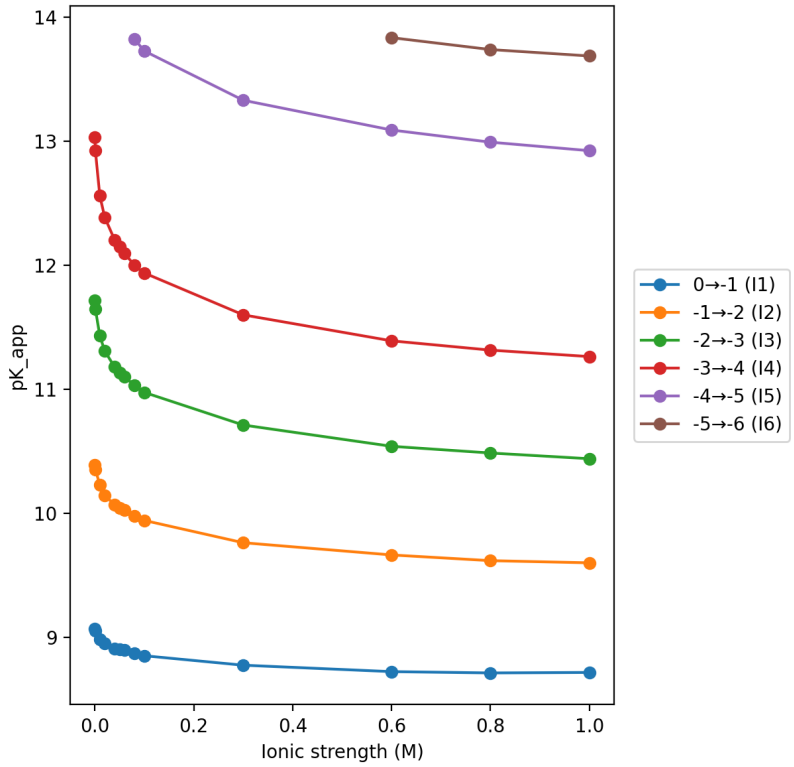

Figure 8: $pK_a^{app}(I)$ values for successive tetramer deprotonation steps plotted against ionic strength.

Funded by the European Union

Funded by the European Union. Views and opinions expressed are however those of the author(s) only and do not necessarily reflect those of the European Union or the European Research Executive Agency (REA). Neither the European Union nor the granting authority can be held responsible for them.

8 Thermodynamic database

The macroscopic $\mathrm{p}K_{\mathrm{a}}^{\mathrm{app}}(I)$ values obtained from Monte Carlo were then used to construct ionic strength dependent effective dissociation constants $\mathrm{p}K_{\mathrm{a}}^{\mathrm{eff}}(I)$ for the oligomers, which are required for PHREEQC/CEMDATA. Using these calibrated $\mathrm{p}K_{\mathrm{a}}^{\mathrm{eff}}(I)$ values, PHREEQC yields the same distribution of species as the Monte Carlo model across all tested ionic strengths and for all oligomers. The tetramer species distributions at 0.6 M is shown in Fig. 9 as an example. This agreement shows that once the intramolecular interaction term extracted from the Monte Carlo simulations is effectively included in $\mathrm{p}K_{\mathrm{a}}^{\mathrm{eff}}(I)$, the continuum PHREEQC model reproduces the same speciation behaviour.

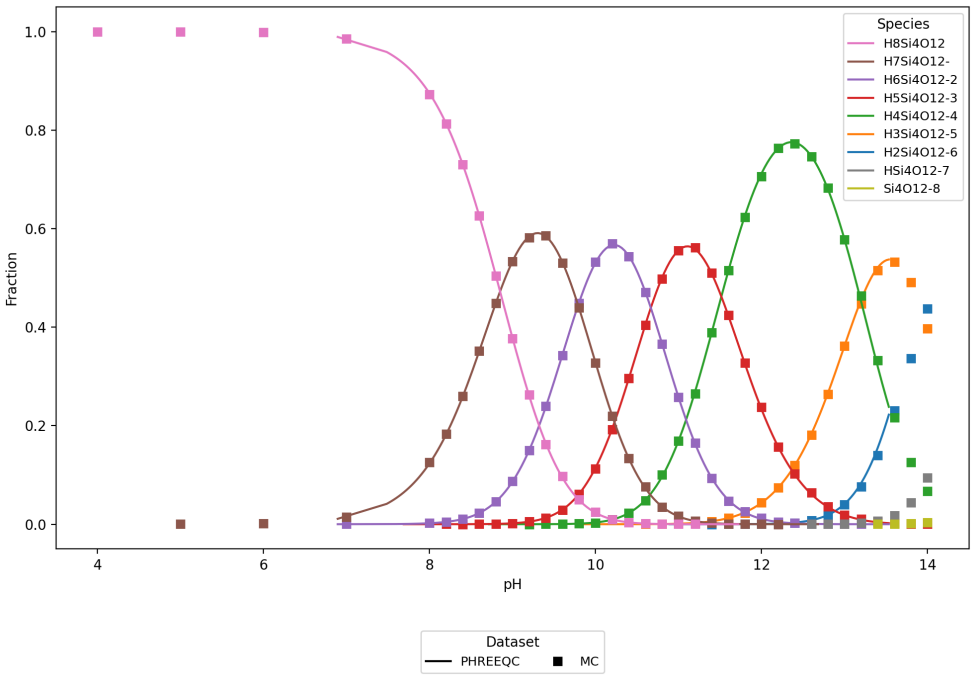

Figure 9: Distribution of tetramer species in 0.6 M NaCl: Monte Carlo vs. PHREEQC.

For incorporation into a general thermodynamic database, the $\mathrm{p}K_{\mathrm{a}}^{\mathrm{eff}}(I)$ curves, were fitted using an extended Debye–Hückel like expression of the form

$$\mathrm{p}K_{\mathrm{a}}^{\mathrm{eff}}(I) = \mathrm{p}K_0 + A\,\frac{\sqrt{I}}{1+\sqrt{I}} + B\,I + C\,I^2 + D\,I^3. \tag{1}$$

Funded by the European Union

Funded by the European Union. Views and opinions expressed are however those of the author(s) only and do not necessarily reflect those of the European Union or the European Research Executive Agency (REA). Neither the European Union nor the granting authority can be held responsible for them.

The obtained $pK_a^{eff}(I)$ for the silicate tetramer together with the fits are illustrated in Fig. 10. Table 3 provides the analytical fit parameters for the $pK_a^{eff}(I)$ of all studied silicate oligomers. The computed parametrized thermodynamic database was validated against silicate speciation experiments, see Appendix A.1.

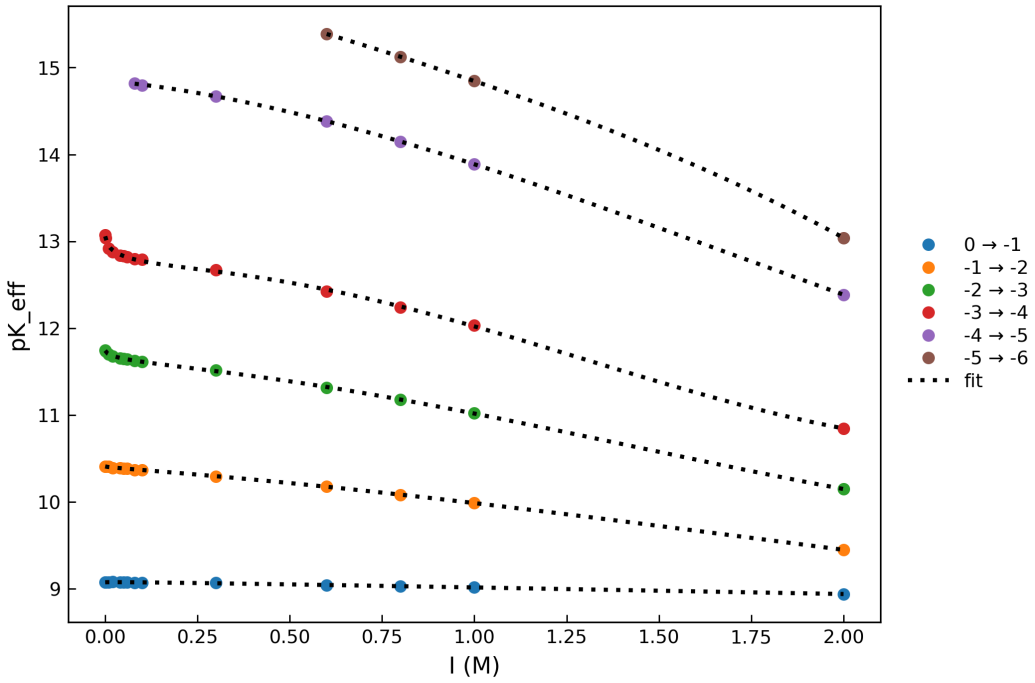

Figure 10: Effective dissociation constants $pK_a^{eff}(I)$ and analytical fits for the tetramer deprotonation steps.

Funded by the European Union

Funded by the European Union. Views and opinions expressed are however those of the author(s) only and do not necessarily reflect those of the European Union or the European Research Executive Agency (REA). Neither the European Union nor the granting authority can be held responsible for them.

Table 3: Fitted parameters ($\mathrm{p}K_0, A, B, C, D$) for the monomer, dimer, linear trimer, cyclic trimer and cyclic tetramer deprotonation reactions (see Appendix A.2 for standard errors and fit quality).

Molecule	Reaction	$\mathrm{p}K_0$	A	B	C	D
monomer	$\mathrm{H_4SiO_4} = \mathrm{H_3SiO_4^-} + \mathrm{H^+}$	9.835	−0.047	0.011	−0.019	0.005
	$\mathrm{H_3SiO_4^-} = \mathrm{H_2SiO_4^{2-}} + \mathrm{H^+}$	13.334	−0.292	−0.350	−0.115	0.020
dimer	$\mathrm{H_6Si_2O_7} = \mathrm{H_5Si_2O_7^-} + \mathrm{H^+}$	9.416	−0.021	−0.021	−0.061	0.017
	$\mathrm{H_5Si_2O_7^-} = \mathrm{H_4Si_2O_7^{2-}} + \mathrm{H^+}$	11.054	−0.167	−0.296	−0.127	0.020
	$\mathrm{H_4Si_2O_7^{2-}} = \mathrm{H_3Si_2O_7^{3-}} + \mathrm{H^+}$	13.963	−0.972	0.103	−0.698	0.169
	$\mathrm{H_3Si_2O_7^{3-}} = \mathrm{H_2Si_2O_7^{4-}} + \mathrm{H^+}$	14.398	3.010	−1.895	0.372	−0.099
linear trimer	$\mathrm{H_8Si_3O_{10}} = \mathrm{H_7Si_3O_{10}^-} + \mathrm{H^+}$	9.112	0.021	−0.078	−0.005	0.001
	$\mathrm{H_7Si_3O_{10}^-} = \mathrm{H_6Si_3O_{10}^{2-}} + \mathrm{H^+}$	10.378	−0.062	−0.238	−0.193	0.042
	$\mathrm{H_6Si_3O_{10}^{2-}} = \mathrm{H_5Si_3O_{10}^{3-}} + \mathrm{H^+}$	11.863	−0.632	0.013	−0.597	0.138
	$\mathrm{H_5Si_3O_{10}^{3-}} = \mathrm{H_4Si_3O_{10}^{4-}} + \mathrm{H^+}$	14.175	−1.115	0.296	−1.011	0.233
	$\mathrm{H_4Si_3O_{10}^{4-}} = \mathrm{H_3Si_3O_{10}^{5-}} + \mathrm{H^+}$	14.945	−0.156	−0.171	−0.879	0.191
cyclic trimer	$\mathrm{H_6Si_3O_9} = \mathrm{H_5Si_3O_9^-} + \mathrm{H^+}$	9.356	−0.017	−0.037	−0.021	0.002
	$\mathrm{H_5Si_3O_9^-} = \mathrm{H_4Si_3O_9^{2-}} + \mathrm{H^+}$	10.865	−0.097	−0.319	−0.085	0.004
	$\mathrm{H_4Si_3O_9^{2-}} = \mathrm{H_3Si_3O_9^{3-}} + \mathrm{H^+}$	12.378	−0.660	−0.016	−0.566	0.129
	$\mathrm{H_3Si_3O_9^{3-}} = \mathrm{H_2Si_3O_9^{4-}} + \mathrm{H^+}$	14.612	−0.025	−0.598	−0.345	0.062
cyclic tetramer	$\mathrm{H_8Si_4O_{12}} = \mathrm{H_7Si_4O_{12}^-} + \mathrm{H^+}$	9.077	0.025	−0.064	−0.010	0.002
	$\mathrm{H_7Si_4O_{12}^-} = \mathrm{H_6Si_4O_{12}^{2-}} + \mathrm{H^+}$	10.411	−0.056	−0.266	−0.158	0.030
	$\mathrm{H_6Si_4O_{12}^{2-}} = \mathrm{H_5Si_4O_{12}^{3-}} + \mathrm{H^+}$	11.748	−0.512	−0.048	−0.550	0.125
	$\mathrm{H_5Si_4O_{12}^{3-}} = \mathrm{H_4Si_4O_{12}^{4-}} + \mathrm{H^+}$	13.073	−1.521	0.798	−1.444	0.356
	$\mathrm{H_4Si_4O_{12}^{4-}} = \mathrm{H_3Si_4O_{12}^{5-}} + \mathrm{H^+}$	14.838	0.087	−0.488	−0.630	0.124
	$\mathrm{H_3Si_4O_{12}^{5-}} = \mathrm{H_2Si_4O_{12}^{6-}} + \mathrm{H^+}$	15.300	3.044	−2.330	0.550	−0.199

For practical use, the fitted parameters are distributed together with a single utility script. The script prompts the user for an ionic strength and returns the corresponding $\mathrm{p}K_{\mathrm{a}}^{\mathrm{eff}}(I)$ values for all silicate deprotonation reactions and also the oligomerization constants which are fitted to match experimental values [2]. It also writes a PHREEQC-ready reaction block containing the associated effective $\log K$ values, allowing users to perform PHREEQC calculations at any chosen ionic strength without rerunning the Monte Carlo simulations. The script and parameter file are available in a DOI-archived repository [20] (DOI: 10.5281/zenodo.17791184).

Funded by the European Union

Funded by the European Union. Views and opinions expressed are however those of the author(s) only and do not necessarily reflect those of the European Union or the European Research Executive Agency (REA). Neither the European Union nor the granting authority can be held responsible for them.

9 Conclusions

This study established a framework in which a microscopic model, solved using Monte Carlo simulations, quantifies the deprotonation reaction of silicate oligomers in electrolyte solutions and transfers this information to continuum speciation models.

The simulations yielded $\mathrm{p}K_{\mathrm{a}}^{\mathrm{app}}(I)$ values for dissolved silica species ranging from the monomer to four unit oligomers across relevant ionic strengths which can be directly compare with experimental data. The simulations captured systematic decrease in acidity with increasing ionic strength, consistent with bulk electrolyte screening.

The large variation in experimentally reported apparent pK values is primarily linked to differences in analytical methods, ionic media, and solution conditions. Standard geochemical models represent each oligomer as a single point like species. They therefore cannot include the intramolecular electrostatic free energy penalty that develops when molecules (here polysilicates) bear multiple negative charges. This missing contribution has prevented consistent fitting of oligomer acid dissociation constants and has limited the use of PHREEQC and similar tools for detailed silicate speciation.

The $\mathrm{p}K_{\mathrm{a}}^{\mathrm{eff}}(I)$ tables for the different silicate species generated here provide a physically grounded and transferable basis for computing silicate activities and speciation in the SiO_2-CaO-Al_2O_3-H_2O system. This supports quantitative modeling of the carbonation behaviour of C-(A)-S-H.

Funded by the European Union

Funded by the European Union. Views and opinions expressed are however those of the author(s) only and do not necessarily reflect those of the European Union or the European Research Executive Agency (REA). Neither the European Union nor the granting authority can be held responsible for them.

References

[1] C. Labbez and B. Jönsson. A new monte carlo method for the titration of molecules and minerals. In *Progress in Colloid and Polymer Science*, volume 133, pages 66–72. Springer, Berlin, 2006.

[2] S. Sjöberg, I. L. Svensson, L.-O. Öhman, and N. Ingri. Equilibrium and structural studies of silicon(iv) and aluminum(iii) in aqueous solution. ii. polysilicate formation in alkaline aqueous solution (a potentiometric and ^{29}si nmr study). *Acta Chemica Scandinavica*, 39:93–107, 1985.

[3] I. L. Svensson, S. Sjöberg, and L.-O. Öhman. Polysilicate equilibria in concentrated sodium silicate solutions. *Journal of the Chemical Society, Faraday Transactions 1*, 82:3635–3646, 1986.

[4] P. S. Roller and G. Ervin. The system calcium oxide–silica–water at 30°c. the association of silicate ion in dilute alkaline solution. *Journal of the American Chemical Society*, 62:461–471, 1940.

[5] G. Lagerström. Equilibrium studies of polyanions. 4. polysilicate equilibria in 1.0 m $naclo_4$ at 25°c. *Acta Chemica Scandinavica*, 13:722–736, 1959.

[6] N. Ingri, G. Lagerström, and L. G. Sillén. Equilibrium studies of polyanions. 3. silicate equilibria in 1.0 m $naclo_4$ at 25°c. *Acta Chemica Scandinavica*, 13:727–735, 1959.

[7] C. F. Baes and R. E. Mesmer. *The Hydrolysis of Cations*. Wiley–Interscience, New York, 1976.

[8] K. R. Applin. The diffusion of dissolved silica. *Geochimica et Cosmochimica Acta*, 51:2147–2151, 1987.

[9] I. Grenthe et al. *Chemical Thermodynamics of Uranium*. Elsevier Science Publishers B.V. for the OECD Nuclear Energy Agency, 1992.

[10] Y. Xiong, C. A. Pelton, and C. Huang. Thermodynamic modeling of aqueous silica solubility in nacl solutions to high temperatures. *Geochimica et Cosmochimica Acta*, 120:1–16, 2013.

Funded by the European Union

Funded by the European Union. Views and opinions expressed are however those of the author(s) only and do not necessarily reflect those of the European Union or the European Research Executive Agency (REA). Neither the European Union nor the granting authority can be held responsible for them.

[11] F. Gaboriaud, A. Nonat, D. Chaumont, and A. Craievich. Aggregation and gel formation in basic silico–calco–alkaline solutions: A saxs, sans, and els study. *The Journal of Physical Chemistry B*, 103(28):5775–5781, 1999.

[12] A. R. Felmy, M. J. Mason, and D. Rai. The solubility of amorphous silica in nacl solutions. *Geochimica et Cosmochimica Acta*, 63:1805–1813, 1999.

[13] Z. Abbas, E. Ahlberg, and S. Nordholm. Monte carlo simulations of salt solutions: Exploring the validity of primitive models. *J. Phys. Chem. B*, 113(18):5905–5916, 2009.

[14] B. Stenqvist, C. Lund, A. Persson, M. Lund, and B. Jönsson. Faunus: A flexible framework for monte carlo simulations. *Molecular Simulation*, 39(14–15):1233–1239, 2013.

[15] M. Lund, B. Jönsson, and T. Äkesson. Protein titration curves in implicit solvent from monte carlo simulations. *Source Code for Biology and Medicine*, 3:1, 2008.

[16] H. S. Harned and G. E. Mannweiler. The thermodynamics of ionized water in sodium chloride solutions. *Journal of the American Chemical Society*, 57:1873–1876, 1935.

[17] H. Bilinski and N. Ingri. Equilibrium studies of polyanions. part ii. polysilicate equilibria in 1.0 m $naclo_4$ at 20°c. *Acta Chemica Scandinavica*, 21:271–280, 1967.

[18] S. Sjöberg, G. Olofsson, and N. Ingri. Activity coefficients for orthosilicic acid and monosilicate ions in 1.0 m kno_3 at 25°c. *Acta Chemica Scandinavica*, 37:153–162, 1983.

[19] N. Näsanen and P. Meriläinen. Thermodynamic properties of lead hydroxide iodide pb(oh)i. *Suomen Kemistilehti B*, 33:149–154, 1960.

[20] Jeswin Jiji and Christophe Labbez. Thermodynamic database for silicate species in aqueous sodium salt solution at 298 k and 1 atm, December 2025. Version 1, Zenodo, https://doi.org/10.5281/zenodo.17791184.

Funded by the European Union

Funded by the European Union. Views and opinions expressed are however those of the author(s) only and do not necessarily reflect those of the European Union or the European Research Executive Agency (REA). Neither the European Union nor the granting authority can be held responsible for them.

A Appendix

A.1 Comparison of PHREEQC Speciation with Potentiometric and ^{29}Si NMR Data

Independent validation was performed by comparing the silicate speciation calculated with PHREEQC using the Monte Carlo derived $pK_a^{\text{eff}}(I)$ values, with experimental silicate speciation studied by potentiometric titration and ^{29}Si MAS NMR on silicate solutions at various concentrations and pH and at 0.6 M NaCl[2]. The experimental and simulated results are compared in Table 4. The PHREEQC results reproduce both the experimentally measured average charge per silicate unit and the distribution of molecular species within experimental uncertainty.

Table 4: Experimental and PHREEQC values for average charge and species concentrations at selected total silicate concentrations. Units in mmol L^{-1}.

$[Si]_{tot}$	$-\log(H^+)$	Z_{exp}	Z_{sim}	$H_3SiO_4^-$		$H_4Si_2O_7^{2-}$		$H_3Si_3O_9^{3-}$	
				Exp.	Sim.	Exp.	Sim.	Exp.	Sim.
38.4	11.60	1.012	1.02680	14.8	13.7997	1.8	2.1984	0.3	0.4475
37.2	11.30	0.980	0.97773	13.0	13.3178	1.5	2.0488	0.2	0.4029
27.5	11.16	0.981	0.96276	10.6	11.2885	1.0	1.4746	0.2	0.2467
22.0	12.02	1.084	1.16302	11.0	9.8831	1.1	1.1309	0.1	0.1658
20.3	11.99	1.064	1.15765	12.2	9.4693	1.0	1.0385	0.2	0.1460
15.6	11.56	1.048	1.05241	6.9	8.4784	0.4	0.8332	–	0.1050
10.0	11.26	1.016	1.01037	5.5	6.3962	0.3	0.4746	–	0.0452
9.4	11.68	1.039	1.09969	5.7	6.0137	0.3	0.4196	–	0.0376

Funded by the European Union

Funded by the European Union. Views and opinions expressed are however those of the author(s) only and do not necessarily reflect those of the European Union or the European Research Executive Agency (REA). Neither the European Union nor the granting authority can be held responsible for them.

A.2 Standard errors and fit quality

Table 5: Standard errors of the fitted parameters (pK_0, A, B, C, D), the residual standard deviation σ_{fit} and the coefficient of determination R^2 for the deprotonation reactions in Table 3.

Molecule	Reaction	σ_{pK_0}	σ_A	σ_B	σ_C	σ_D	σ_{fit}	R^2
monomer	$H_4SiO_4 \rightarrow H_3SiO_4^- + H^+$	0.002	0.017	0.024	0.028	0.009	0.002	0.974
	$H_3SiO_4^- \rightarrow H_2SiO_4^{2-} + H^+$	0.003	0.026	0.038	0.045	0.014	0.004	1.000
dimer	$H_6Si_2O_7 \rightarrow H_5Si_2O_7^- + H^+$	0.002	0.018	0.026	0.030	0.010	0.002	0.998
	$H_5Si_2O_7^- \rightarrow H_4Si_2O_7^{2-} + H^+$	0.003	0.032	0.046	0.053	0.017	0.004	0.999
	$H_4Si_2O_7^{2-} \rightarrow H_3Si_2O_7^{3-} + H^+$	0.005	0.043	0.063	0.073	0.024	0.006	0.999
linear trimer	$H_8Si_3O_{10} \rightarrow H_7Si_3O_{10}^- + H^+$	0.002	0.015	0.022	0.026	0.008	0.002	0.998
	$H_7Si_3O_{10}^- \rightarrow H_6Si_3O_{10}^{2-} + H^+$	0.002	0.021	0.030	0.035	0.011	0.003	0.999
	$H_6Si_3O_{10}^{2-} \rightarrow H_5Si_3O_{10}^{3-} + H^+$	0.004	0.037	0.053	0.062	0.020	0.005	0.999
	$H_5Si_3O_{10}^{3-} \rightarrow H_4Si_3O_{10}^{4-} + H^+$	0.023	0.183	0.197	0.198	0.061	0.012	0.999
	$H_4Si_3O_{10}^{4-} \rightarrow H_3Si_3O_{10}^{5-} + H^+$	0.057	0.332	0.246	0.191	0.051	0.005	1.000
cyclic trimer	$H_6Si_3O_9 \rightarrow H_5Si_3O_9^- + H^+$	0.003	0.025	0.036	0.042	0.013	0.003	0.995
	$H_5Si_3O_9^- \rightarrow H_4Si_3O_9^{2-} + H^+$	0.003	0.028	0.041	0.047	0.015	0.004	1.000
	$H_4Si_3O_9^{2-} \rightarrow H_3Si_3O_9^{3-} + H^+$	0.005	0.045	0.065	0.075	0.024	0.006	1.000
	$H_3Si_3O_9^{3-} \rightarrow H_2Si_3O_9^{4-} + H^+$	0.110	0.678	0.532	0.429	0.118	0.013	1.000
cyclic tetramer	$H_8Si_4O_{12} \rightarrow H_7Si_4O_{12}^- + H^+$	0.003	0.025	0.036	0.041	0.013	0.003	0.995
	$H_7Si_4O_{12}^- \rightarrow H_6Si_4O_{12}^{2-} + H^+$	0.003	0.028	0.041	0.047	0.015	0.004	1.000
	$H_6Si_4O_{12}^{2-} \rightarrow H_5Si_4O_{12}^{3-} + H^+$	0.004	0.035	0.051	0.059	0.019	0.005	1.000
	$H_5Si_4O_{12}^{3-} \rightarrow H_4Si_4O_{12}^{4-} + H^+$	0.014	0.134	0.194	0.226	0.073	0.018	0.999
	$H_4Si_4O_{12}^{4-} \rightarrow H_3Si_4O_{12}^{5-} + H^+$	0.078	0.452	0.335	0.260	0.070	0.006	1.000

Funded by the European Union

Funded by the European Union. Views and opinions expressed are however those of the author(s) only and do not necessarily reflect those of the European Union or the European Research Executive Agency (REA). Neither the European Union nor the granting authority can be held responsible for them.